STEADY-STATE PERFORMANCE OF MULTICHANNEL AFFINE PROJECTION ALGORITHMS FOR ACTIVE NOISE CONTROL

Miguel Ferrer, Alberto Gonzalez, Maria de Diego and Gema Piñero

Institute of Telecommunications and Multimedia Applications (iTEAM)
Universidad Politecnica de Valencia
phone: + (34) 963879763, email: mferrer@dcom.upv.es
web: www.iteam.upv.es

ABSTRACT

In the field of adaptive filtering, it is well known that affine projection (AP) algorithms lead to a good tradeoff between convergence speed and computational load. For multichannel sound control, some computationally efficient AP (fast AP) algorithms have been recently proposed. This paper analyzes the steady-state mean square error of two efficient affine projection algorithms (representative of the different approaches) for multichannel active noise control (ANC) applications based on a different filtering-x scheme: the modified filtered-x affine projection (MFXAP) algorithm (with the modified filtered-x structure embedded) and the filtered-x affine projection (FXAP) algorithm (based on the conventional filtered-x structure). This study depends on energy conservation arguments and does not require a specific signal distribution. The theoretical models derived allow to accurately predict the steady-state performance of the algorithms considered. Simulation results obtained in practical single-channel and multichannel ANC systems validate the analysis and the derived expressions.

1. INTRODUCTION

In adaptive signal applications, the LMS family is a widely used adaptive algorithms type due to its simplicity and computational effort [1]. However, in recent years, the affine projection (AP) algorithms and their efficient approaches proposed with the main purpose of speeding the convergence speed of the LMS type algorithms as well as to reduce the computational load have become a meaningful alternative to other adaptive algorithms developed to address the slow convergence speed of the LMS algorithms as the recursive least square (RLS) type algorithms [2]. Therefore, AP algorithms exhibit good convergence properties and robustness in practical implementations with moderate computational effort. In multichannel sound control applications, most of the AP algorithms, including their computationally efficient versions, are used with the modified filtered-x structure [3], see Fig. 1(a). However, the AP algorithms can also be based on the conventional filtered-x structure (see Fig. 1(b)) (FXAP algorithm) [4] that is less demanding from a computational cost point of view than the approaches based on the modified filtered-x scheme, named MFXAP algorithms, especially for multichannel systems.

In this paper, following an approach similar to [5] and adapting it to multichannel filtered-x AP algorithms for ANC, the steady-state mean square error of the MFXAP and the FXAP algorithms for multichannel active noise controllers is analyzed and some theoretical models are developed in order to predict the algorithms performance. Section II reports a brief description of the single channel and multichannel AP algorithms considered. In Section III the theoretical models for the MSE of the FXAP and the MFXAP (previously analyzed in [6]), are derived. Section IV provides some simulation results of an ANC system that validate the analytical predictions. Conclusions are included in Section V.

Partially supported by: CICYT grant TEC2006-13883-C04-01.

2. FILTERED-X AFFINE PROJECTION ALGORITHMS

2.1 Single-channel filtered-x AP algorithms

The update equation of the AP adaptive filter coefficients in the single-channel case reads as:

$$\mathbf{w}_L(n) = \mathbf{w}_L(n-1) - \mu \mathbf{V}^T(n)[\mathbf{V}(n)\mathbf{V}^T(n) + \delta \mathbf{I}]^{-1}\mathbf{e}_N(n), \quad (1)$$

where δ is a regularization parameter, $\mathbf{I}$ is a $N \times N$ identity matrix, μ is a convergence parameter and $\mathbf{e}_N(n)$ is called the error vector. Moreover, $\mathbf{w}_L(n)$ is a vector comprised of the L adaptive filter coefficients at the nth time instant. Matrix $\mathbf{V}(n)$ of dimensions $N \times L$ contains the filtered reference signal values as follows:

$$\mathbf{V}^T(n) = [\mathbf{v}(n), \mathbf{v}(n-1), ..., \mathbf{v}(n-N+1)], \quad (2)$$

where $\mathbf{v}(n)$ is a vector with the more recent L samples of the reference signal $x(n)$ filtered through a version $\hat{h}$ of the secondary path, and N is called the AP order [2]. The objective is to estimate the L-dimensional optimal coefficient vector $\mathbf{w}_L^o$, such that the desired signal vector was given by $\mathbf{d}_N(n) = -\mathbf{V}(n)\mathbf{w}_L^o$. However, this result is not achieved in practice and it is more realistic to use,

$$\mathbf{d}_N(n) = -\mathbf{V}(n)\mathbf{w}_L^o + \mathbf{r}_N(n) \quad (3)$$

being $\mathbf{r}_N(n)$ a $N \times 1$ Gaussian noise vector of zero mean and σ_r^2 variance, uncorrelated with data signal.

In case of the modified filtered-x affine projection (MFXAP) algorithm based on the modified filtered-x scheme (see Fig. 1(a)), the error vector is obtained as $\mathbf{e}_N(n) = \mathbf{d}_N(n) + \mathbf{V}(n)\mathbf{w}_L(n-1)$. However, the FXAP algorithm, based on the conventional filtered-x structure (see Fig. 1(b)), builds the error vector with past samples of the error signal $e(n)$, $\mathbf{e}_N(n) \approx [e(n), e(n-1), ..., e(n-N+1)]^T$. This error vector approximation is accurate in most cases. In such a case, both algorithms, the MFXAP and the FXAP can exhibit a similar performance (see [4] for more details regarding efficient AP algorithms description).

2.2 Multichannel filtered-x AP algorithms

Whereas a single-channel controller uses only one reference sensor, one secondary source and one error sensor, a multichannel system is comprised of I reference signals, J secondary sources and K error sensors. Therefore, the multichannel extension of AP algorithms involves expanding the matrices and vectors considered in (1) that becomes,

$$\mathbf{w}(n) = \mathbf{w}(n-1) - \mu \mathbf{V}(n)[\mathbf{V}^T(n)\mathbf{V}(n) + \delta \mathbf{I}]^{-1}\mathbf{e}(n), \quad (4)$$

being now $\mathbf{I}$ a $KN \times KN$ identity matrix and $\mathbf{w}(n)$ a IJL vector with the coefficients of the IJ adaptive filters arranged as follows,

$$\mathbf{w}(n) = [\mathbf{w}_{1,1}^T(n), \ldots \mathbf{w}_{1,I}^T(n), \mathbf{w}_{2,1}^T(n), \ldots, \mathbf{w}_{J,I}^T(n)]^T \quad (5)$$

where $\mathbf{w}_{j,i}(n)$ is a vector with the L coefficients of the adaptive filter that connects the ith primary signal with the jth secondary source.

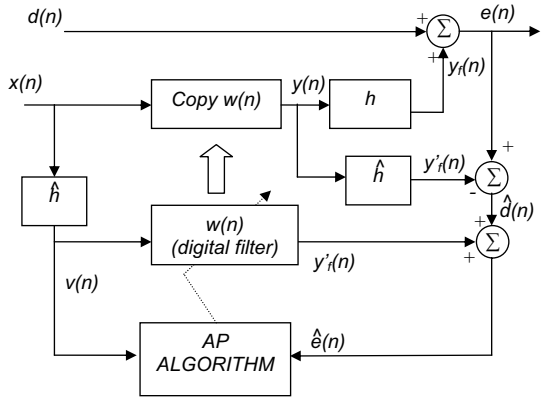

(a)

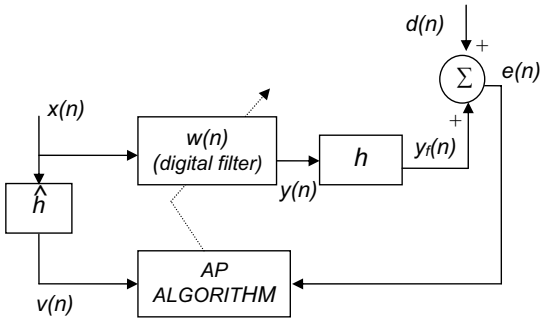

(b)

Figure 1: Block diagram of an adaptive system using: (a) the modified filtered-x structure and (b) the conventional filtered-x structure.

$\mathbf{e}(n)$ is the KN error vector with the last N samples of each error sensor, $\mathbf{e}(n) = [e_1(n),\ldots,e_1(n-N+1),\ldots,e_K(n),\ldots,e_K(n-N+1)]^T$. Finally, the $(IJL \times KN)$ matrix $\mathbf{V}(n)$ is given by $[\mathbf{V}_1(n)\ldots\mathbf{V}_K(n)]$, where the matrices $\mathbf{V}_k(n)$ of $(IJL \times N)$ dimensions are comprised of the reference signal samples in the following way,

$$\mathbf{V}_k(n) = \begin{pmatrix} \mathbf{v}_{1,1,k}(n) & \ldots & \mathbf{v}_{1,1,k}(n-N+1) \\ & \vdots & \\ \mathbf{v}_{I,1,k}(n) & \ldots & \mathbf{v}_{I,1,k}(n-N+1) \\ & \vdots & \\ \mathbf{v}_{1,J,k}(n) & \ldots & \mathbf{v}_{1,J,k}(n-N+1) \\ & \vdots & \\ \mathbf{v}_{I,J,k}(n) & \ldots & \mathbf{v}_{I,J,k}(n-N+1) \end{pmatrix}, \quad (6)$$

where $\mathbf{v}_{i,j,k}(n)$ is the filtered-x vector of L length obtained by filtering, sample by sample, the ith reference signal $x_i(n)$ with the secondary path estimation between the jth secondary source and the kth error sensor: $\mathbf{v}_{i,j,k}(n) = [v_{i,j,k}(n), v_{i,j,k}(n-1),\ldots,v_{i,j,k}(n-L+1)]^T$.

On the other hand, the multichannel error is defined as

$$e_M(n) = \sum_{k=1}^{K} e_k(n) = \sum_{k=1}^{K} [d_k(n) + \mathbf{v}_k(n)^T \mathbf{w}(n-1)] \quad (7)$$

where $e_k(n)$ and $d_k(n)$ are the error signal and the reference signal, respectively, at the kth error sensor. Moreover, $\mathbf{v}_k(n)$ is the $IJL \times 1$ data vector

$$\mathbf{v}_k(n) = [\mathbf{v}_{1,1,k}(n)^T,\ldots,\mathbf{v}_{I,1,k}(n)^T,\ldots,\mathbf{v}_{1,J,k}(n)^T,\ldots,\mathbf{v}_{I,J,k}(n)^T]^T. \quad (8)$$

By introducing the $N \times NK$ matrix $\mathbf{D}_{NK} = [I, I, ..., I]$, which consists of K identity matrices of $N \times N$ size, we can define the multichannel error vector as,

$$\mathbf{e}_N(n) = \mathbf{D}_{NK}\mathbf{e}(n) \quad (9)$$

that will be used for the algorithm analysis, being the multichannel error $e_M(n)$ the first element of $\mathbf{e}_N(n)$.

2.2.1 Multichannel MFXAP

In case we consider the multichannel MFXAP, based on the modified filtered-x structure illustrated in Fig.1(a), the error vector $\mathbf{e}(n)$ for the multichannel MFXAP is defined as

$$\mathbf{e}(n) = \mathbf{d}(n) + \mathbf{V}^T(n)\mathbf{w}(n-1) \quad (10)$$

where $\mathbf{d}(n)$ is a NK column vector comprised of the last N samples of the desired signal at each error sensor,

$$\mathbf{d}(n) = [d_1(n),\ldots,d_1(n-N+1),\ldots,d_K(n),\ldots,d_K(n-N+1)]^T. \quad (11)$$

From (9), we can rewrite (10) as

$$\mathbf{e}_N(n) = \mathbf{d}_N(n) + \overline{\mathbf{V}}(n)^T\mathbf{w}(n-1) \quad (12)$$

where $\mathbf{d}_N(n)$ is a vector of N length built as the addition of K vectors comprised of the last N samples of the reference signals. The $IJL \times N$ matrix $\overline{\mathbf{V}}(n) = \mathbf{V}(n)\mathbf{D}_{NK}^T$ is the addition of the K matrices $\mathbf{V}_k(n)$ defined in (6).

The objective of the multichannel adaptive algorithm is analogous to that of the single channel case described in [4]. That is, to estimate the optimal coefficient vector $\mathbf{w}^o$ of IJL length given by

$$\mathbf{d}(n) = -\mathbf{V}^T(n)\mathbf{w}^o + \mathbf{r}(n) \quad (13)$$

being $\mathbf{r}(n)$ a $KN \times 1$ Gaussian noise vector uncorrelated with data signals and comprised of the biases at each error sensor, $\mathbf{r}(n) = [\mathbf{r}_1^T(n), \mathbf{r}_2^T(n),\ldots,\mathbf{r}_K^T(n)]^T$.

By premultiplying both sides of (13) by $\mathbf{D}_{NK}$ it follows that

$$\mathbf{d}_N(n) = -\overline{\mathbf{V}}^T(n)\mathbf{w}^o + \mathbf{r}_N(n) \quad (14)$$

being $\mathbf{r}_N(n)$ the addition of the K vectors $\mathbf{r}_k(n)$.

If we take into account $\mathbf{e}_N(n)$ and $\overline{\mathbf{V}}(n)$ defined in (12), an approximate version of the multichannel MFXAP [6] can be derived from (4)

$$\mathbf{w}'(n) = \mathbf{w}'(n-1) - \mu\overline{\mathbf{V}}(n)[\overline{\mathbf{V}}^T(n)\overline{\mathbf{V}}(n) + \delta\mathbf{I}]^{-1}\mathbf{e}_N(n) \quad (15)$$

where now, $\mathbf{I}$ is an $N \times N$ identity matrix. Note that the derived equation (15) can be understood as if the multichannel system considers only an error sensor equivalent to the contribution of the K error sensors in the multichannel system. Then, the coefficient error vector of IJL length is given by

$$\widetilde{\mathbf{w}}(n) = \mathbf{w}^o - \mathbf{w}'(n), \quad (16)$$

and from (15) it holds

$$\widetilde{\mathbf{w}}(n) = \widetilde{\mathbf{w}}(n-1) + \mu\overline{\mathbf{V}}(n)[\overline{\mathbf{V}}^T(n)\overline{\mathbf{V}}(n) + \delta\mathbf{I}]^{-1}\mathbf{e}_N(n). \quad (17)$$

From (16), we can define the multichannel *a priori* and *a posteriori* error vectors

$$\mathbf{e}^a(n) = \overline{\mathbf{V}}^T(n)\widetilde{\mathbf{w}}(n-1) \quad (18)$$

and

$$\mathbf{e}^p(n) = \overline{\mathbf{V}}^T(n)\widetilde{\mathbf{w}}(n). \quad (19)$$

2.2.2 Multichannel FXAP

The recently proposed filtered-x affine projection (FXAP) algorithm for multichannel ANC [4] is based on the conventional filtered-x scheme. Following, only the main differences with the multichannel MFXAP algorithm description are remarked. The error vector is now defined as

$$\mathbf{e}_N(n) = \mathbf{d}_N(n) + \begin{pmatrix} \overline{\mathbf{v}}^T(n)\mathbf{w}'(n-1) \\ \overline{\mathbf{v}}^T(n-1)\mathbf{w}'(n-2) \\ \vdots \\ \overline{\mathbf{v}}(n-N+1)\mathbf{w}'(n-N) \end{pmatrix}, \quad (20)$$

that according to (14) allow to define the new *a priori* error vector

$$\mathbf{e}_N^{a'}(n) = \begin{pmatrix} e_M^a(n) \\ e_M^a(n-1) \\ \vdots \\ e_M^a(n-N+1) \end{pmatrix} = \begin{pmatrix} \overline{\mathbf{v}}^T(n)\widetilde{\mathbf{w}}(n-1) \\ \overline{\mathbf{v}}^T(n-1)\widetilde{\mathbf{w}}(n-2) \\ \vdots \\ \overline{\mathbf{v}}^T(n-N+1)\widetilde{\mathbf{w}}(n-N) \end{pmatrix} \quad (21)$$

being $\overline{\mathbf{v}}(n) = \sum_{k=1}^{K} \mathbf{v}_k(n)$. Note that as in [7] we get

$$\mathbf{e}_N(n) = -\mathbf{e}_N^{a'}(n) + \mathbf{r}_N(n). \quad (22)$$

3. STEADY-STATE ANALYSIS

Our objective is to evaluate the steady-state mean square error performance of the multichannel MFXAP and multichannel FXAP algorithms. Then, we estimate the MSE as the limit for $n \to \infty$ of the mean square multichannel error,

$$\text{MSE} = \lim_{n\to\infty} E\{|e_M(n)|^2\}, \quad (23)$$

or equivalently, the excess mean square multichannel error (EMSE) which is defined by

$$\text{EMSE} = \lim_{n\to\infty} E\{|e_M^a(n)|^2\} \quad (24)$$

where $e_M^a(n) = \overline{\mathbf{v}}^T(n)\widetilde{\mathbf{w}}(n-1)$.

Note that the definition of the MSE in (23) refers to the mean square of the sum of the K error signals (see (7)) instead of the sum of the mean square errors. This definition provides a first approximation to the accurate MSE and differs from it by a quantity dependent on the cross products of the different error signals. Then, the estimated MSE provides a lower bound of the exact MSE.

Regarding the FXAP, from (9) and (22) it holds the relation between the MSE and the EMSE,

$$\text{MSE} = \text{EMSE} + K\sigma_r^2, \quad (25)$$

being σ_r^2 the noise variance at each error sensor.

Following the approach shown in [5], a recursion for $||\widetilde{w}(n)||^2$ based on the energy conservation relation can be derived, where $||\cdot||$ denotes the Euclidean norm. Then, suitably manipulating and taking energies at both sides of (15), the energy conservation relation is obtained,

$$\begin{aligned} &\|\widetilde{\mathbf{w}}(n)\|^2 + \mathbf{e}^a(n)^T[\overline{\mathbf{V}}^T(n)\overline{\mathbf{V}}(n)]^{-1}\mathbf{e}^a(n) = \\ &\quad \|\widetilde{\mathbf{w}}(n-1)\|^2 + \mathbf{e}^p(n)^T[\overline{\mathbf{V}}^T(n)\overline{\mathbf{V}}(n)]^{-1}\mathbf{e}^p(n). \end{aligned} \quad (26)$$

Note that the energies of the coefficient error vectors at different iterations are related to the weighted energies of the *a priori* and *a posteriori* error vectors, just as the relation provided in [5]. Applying the expectation operator $E\{\cdot\}$ at both sides of (26) and the steady-state conditions ($E\{\|\widetilde{\mathbf{w}}(n)\|^2\} = E\{\|\widetilde{\mathbf{w}}(n-1)\|^2\}$ as $n \to \infty$), it becomes

$$\begin{aligned} &\mu E\{\mathbf{e}_N^{a'}(n)^T\boldsymbol{\Psi}_M(n)\mathbf{e}_N^{a'}(n)\} + \mu E\{\mathbf{r}_N^T(n)\boldsymbol{\Psi}_M(n)\mathbf{r}_N(n)\} \\ &\quad = 2E\{\mathbf{e}_N^{a'}(n)^T\boldsymbol{\Phi}_M(n)\mathbf{e}^a(n)\}. \end{aligned} \quad (27)$$

For this purpose, we have considered (18), (19) and (22), and the following $N \times N$ data function matrices have been defined

$$\begin{aligned} \boldsymbol{\Phi}_{\mathbf{M}}(n) &= [\overline{\mathbf{V}}^T(n)\overline{\mathbf{V}}(n) + \delta\mathbf{I}]^{-1} \\ \boldsymbol{\Psi}_{\mathbf{M}}(n) &= \boldsymbol{\Phi}_{\mathbf{M}}(n)\overline{\mathbf{V}}^T(n)\overline{\mathbf{V}}(n)\boldsymbol{\Phi}_{\mathbf{M}}(n). \end{aligned} \quad (28)$$

In the analysis of FXAP and MFXAP, we introduce some approximations due to statistical independence considerations between different vectors and matrices. Concretely we assume data function matrices be independent from $\widetilde{\mathbf{w}}(n)$ and the other involved vectors. Moreover, we neglect the dependency between the *a priori* error vector and the noise error vector.

By manipulating (27) and considering the equality for two column vectors of length N, $\mathbf{a}^T\mathbf{b} = Tr(\mathbf{a}\mathbf{b}^T)$, it yields

$$\begin{aligned} &\mu Tr[E\{\mathbf{e}_N^{a'}(n)\mathbf{e}_N^{a'}(n)^T\}E\{\boldsymbol{\Psi}_M(n)\}] \\ &+\mu Tr[E\{\mathbf{r}_N(n)\mathbf{r}_N(n)^T\}E\{\boldsymbol{\Psi}_M(n)\}] \\ &= 2Tr[E\{\mathbf{e}_N^{a'}(n)\mathbf{e}^a(n)^T\}E\{\boldsymbol{\Phi}_M(n)\}]. \end{aligned} \quad (29)$$

Next, some simplifications and assumptions are applied to the different terms in (29). Concretely, in steady-state, when $n \to \infty$, it is found that $E\{|e_M^a(n)|^2\} = E\{|e_M^a(n-1)|^2\} = \ldots = E\{|e_M^a(n-N+1)|^2\}$. Moreover, off-diagonal terms of the $E\{\mathbf{e}_N^{a'}(n)\mathbf{e}_N^{a'}(n)^T\}$ matrix are neglected following [5]. Then, the first term on the left hand side of (29) becomes

$$\begin{aligned} &\mu Tr[E\{\mathbf{e}_N^{a'}(n)\mathbf{e}_N^{a'}(n)^T\}E\{\boldsymbol{\Psi}_M(n)\}] \\ &= \mu E\{|\, e_M^a(n)\,|^2\}Tr[E\{\boldsymbol{\Psi}_M(n)\}], \end{aligned} \quad (30)$$

being $e_M^a(n)$ the top element of the particular *a priori* error vector $\mathbf{e}_N^{a'}(n)$ (see (21)).

The second term, related with the noise vector, simplifies to

$$\mu Tr[E\{\mathbf{r}_N(n)\mathbf{r}_N(n)^T\}E\{\boldsymbol{\Psi}_M(n)\}] = \mu K\sigma_r^2 Tr[E\{\boldsymbol{\Psi}_M(n)\}]. \quad (31)$$

Finally, the term on the right hand side of (29) can be simplified by means of similar considerations. Upon substituting (18), (19) and (22) into (17) when δ is small, we get that

$$\mathbf{e}^p(n) = \mathbf{e}^a(n) + \mu\mathbf{e}_N^{a'}(n) - \mu\mathbf{r}_N(n). \quad (32)$$

Moreover, under the assumption that $\mathbf{r}_N(n)$ is independent with $\mathbf{e}_N^{a'}(n)$, the following relations can be derived,

$$\begin{aligned} &E\{\overline{\mathbf{v}}^T(n)\widetilde{\mathbf{w}}(n-1)\overline{\mathbf{v}}^T(n)\widetilde{\mathbf{w}}(n-1)\} = E\{|e_M^a(n)|^2\}, \\ &E\{\overline{\mathbf{v}}^T(n-1)\widetilde{\mathbf{w}}(n-2)\overline{\mathbf{v}}^T(n-1)\widetilde{\mathbf{w}}(n-1)\} \\ &\qquad = (1-\mu)E\{|e_M^a(n-1)|^2\}, \\ &\quad \vdots \\ &E\{\overline{\mathbf{v}}^T(n-N+1)\widetilde{\mathbf{w}}(n-N)\overline{\mathbf{v}}^T(n-N+1)\widetilde{\mathbf{w}}(n-1)\} \\ &\qquad = [1-(N-1)\mu]E\{|\, e_M^a(n-N+1)\,|^2\}, \end{aligned} \quad (33)$$

that it leads to,

$$E\{\mathbf{e}_N^{a'}(n)\mathbf{e}^a(n)^T\} \approx E\{|\, e_M^a(n)\,|^2\}D_1, \quad (34)$$

where the $N \times N$ diagonal matrix D_1 is given by

$$D_1 = \text{diag}\{1, (1-\mu), (1-2\mu), ..., [1-(N-1)\mu]\}, \quad (35)$$

being diag$\{...\}$ the diagonal matrix of the entries $\{...\}$.

Finally, equation (29) becomes

$$\mu E\{|\, e_M^a(n)\,|^2\} Tr[E\{\mathbf{\Psi}_M(n)\}] + \mu K\sigma_r^2 Tr[E\{\mathbf{\Psi}_M(n)\}] = 2E\{|\, e_M^a(n)\,|^2\} Tr[E\{D_1\mathbf{\Phi}_M(n)\}], \quad (36)$$

and the MSE of the multichannel FXAP is therefore given by

$$\text{MSE} = K\sigma_r^2 + \frac{\mu K\sigma_r^2 Tr[E\{\mathbf{\Psi}_M(n)\}]}{2Tr[E\{D_1\mathbf{\Phi}_M(n)\}] - \mu Tr[E\{\mathbf{\Psi}_M(n)\}]}. \quad (37)$$

This expression can be simplified when the regularization parameter δ is small enough. Then, we get,

$$\text{MSE} = K\sigma_r^2 \left[1 + \frac{\mu Tr[E\{\mathbf{\Psi}_M(n)\}]}{Tr[D_2 E\{\mathbf{\Psi}_M(n)\}]}\right], \quad (38)$$

being $\mathbf{I}$ the $N \times N$ identity matrix and D_2 a diagonal matrix given by

$$D_2 = \text{diag}\{(2-\mu),(2-3\mu),...,[2-(2N-1)\mu]\}. \quad (39)$$

Moreover, another two simplifications can be carried out depending on μ values:

- If μ is small, $D_2 \approx 2I$ and (38) reduces to,

$$\text{MSE} = K\sigma_r^2 \left[1 + \frac{\mu}{2}\right], \quad (40)$$

- If $\mu \approx 1$, then,

$$\text{MSE} = K\sigma_r^2 \left[1 + \mu \frac{Tr([E\{\mathbf{\Psi}_M(n)\}]}{Tr[D_3 E\{\mathbf{\Psi}_M(n)\}]}\right], \quad (41)$$

where

$$D_3 = \text{diag}\{1,-1,\cdots,(3-2N)\}. \quad (42)$$

Note that this expression for the MSE could provide non coherent results due to negative entries in matrix D_3. This agrees well with instabilities found in simulation results for large μ values.

If we take into account the previous expressions and with similar hypothesis to that of the MSE for single-channel MFXAP and FXAP [7], the MSE of the multichannel MFXAP can be derived,

$$\text{MSE} = K\sigma_r^2 + \frac{\mu K\sigma_r^2 Tr(E\{\mathbf{\Psi}_\mathbf{M}(n)\})}{2Tr[E\{D_4\mathbf{\Phi}_\mathbf{M}(n)\}] - \mu Tr[E\{D_4\mathbf{\Psi}_\mathbf{M}(n)\}]}, \quad (43)$$

being

$$D_4 = \text{diag}\{1,(1-\mu)^2,(1-\mu)^4,\cdots,(1-\mu)^{[2(N-1)]}\}. \quad (44)$$

The corresponding estimated MSE for the single-channel algorithms was introduced in [7] and can be derived from the previous expressions with $I = J = K = 1$.

4. SIMULATION RESULTS

In this section, we show several experimental results that compare the theoretical predicted values of the steady-state MSE with values obtained from simulations. We provide results both for a single channel and for a multichannel 1:2:2 ANC system. In the multichannel case, two loudspeakers were used as secondary sources and a third loudspeaker produced a colored Gaussian noise generated by filtering white Gaussian noise (of zero mean and unit variance) with a first order autoregressive filter of transfer function $\sqrt{1-a^2}/(1-az^{-1})$ being $a = 0.9$, as primary signal. The desired signal vector $\mathbf{d}_N(n)$ generated by following the model in (3) or (14), depending on system dimensions, with Gaussian noise of $\sigma_r^2 = 0.001$ and an optimal coefficient vector $\mathbf{w}_L^o$ of 16 coefficients. The secondary path was perfectly model with an 8 coefficients filter, and the adaptive filter has the same length as the unknown channel (16 coefficients).

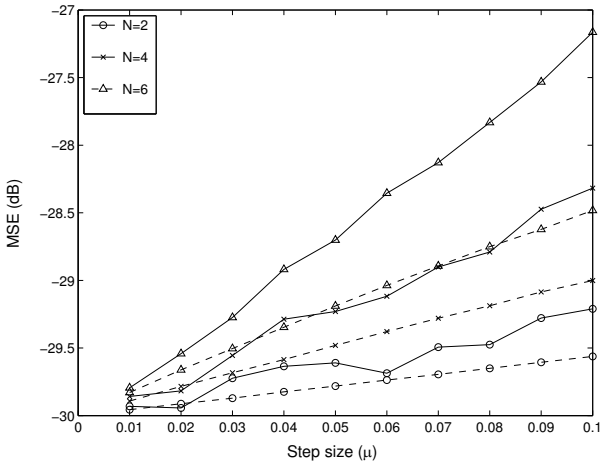

Figure 2: Comparison between the estimated MSE by (38) (dashed line) and the simulated MSE (solid line), as a function of μ for *N=2,4* and 6.

The experimental results of MSE were obtained by averaging over 10 independent runs of 800.000 samples (necessary to arrive at steady-state) with $\delta = 10^{-5}$. In addition, different step size μ and AP orders were applied.

In the first experiment we consider a single-channel ANC system. Fig. 2 diagrams the MSE for the FXAP obtained from simulations or estimated with (38) at different values of the step size μ and for the AP orders *N=2,4,* and 6. The estimated curves lie close to the simulated ones, closer for low μ values and for AP orders of moderate value. Moreover, the MSE worsens when μ increases and higher AP orders speed up this effect for increasing μ. Figure 3(a) illustrates the evolution of the residual error of the FXAP for $N = 3,7$ and $\mu = 0.02$ for the first samples. Each sample of the diagram has been estimated by an exponential window of 100 samples of the residual error power averaged over 10 runs, and only the transient period at the beginning of the adaptation process is shown. It can be observed the good convergence speed the FXAP exhibits, much faster as N increases and very similar to the convergence performance of the MFXAP [4]. In the figure there are also shown the asymptotic values (dotted line) of the residual error (MSE).

The second experiment considers the multichannel ANC system described above. Figure 3(b) shows the multichannel residual errors obtained for both algorithms, the FXAP (solid line) and the MFXAP (dashed line) for $N = 3$ and $\mu = 0.02$ for the first 5000 samples. In both cases, the residual errors lead to the estimated MSE (almost identical for both algorithms) and the convergence speeds are very similar. Fig. 4 diagrams the simulated and the estimated MSE for AP orders $N = 2,3$ and 4, for the step size ranging from 10^{-5} to 0.04. The range of μ values has been chosen in order to guarantee stability of the multichannel FXAP algorithm, unlike higher values would be allowed for the multichannel MFXAP. However, the increase in convergence speed is not worth the computational load requirements for the MFXAP [4]. The comparison between the estimated MSE by (37) and the values obtained by simulation for the FXAP is illustrated in Fig. 4(a). The estimated curves lie closer to the simulated ones for low μ values and $N = 2,3$. Moreover, these theoretical curves are very similar between them because for low μ values the estimated MSE seems not to be dependent on N, see (40). Similar considerations can be applied to Fig. 4(b) that shows the estimated MSE by (43) or the simulation values for the multichannel MFXAP. Moreover, in this case, the estimated curves for low AP orders fall close to the corresponding simulation values with a weaker dependency from μ values. However, in Fig. 4(a)

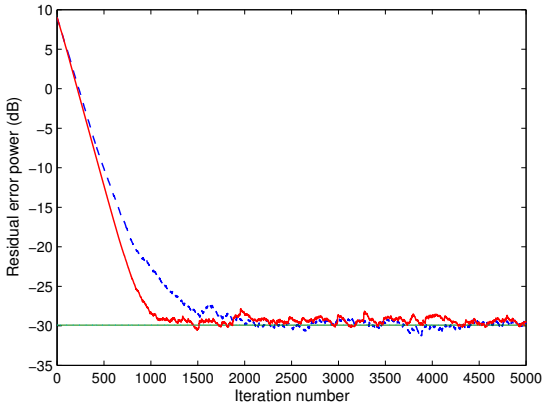

(a)

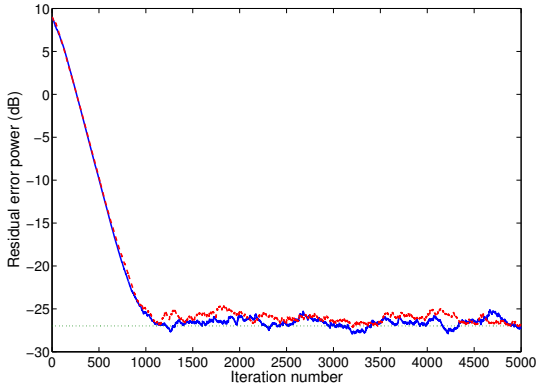

(b)

Figure 3: Evolution of residual error compared with the theoretical MSE value (dotted line) for: (a) the FXAP with $N = 3$ (dashed line) and $N = 7$ (solid line), and (b) the multichannel algorithms MFXAP (dashed line) and FXAP (solid line) with $N = 3$. ($\mu = 0.02$).

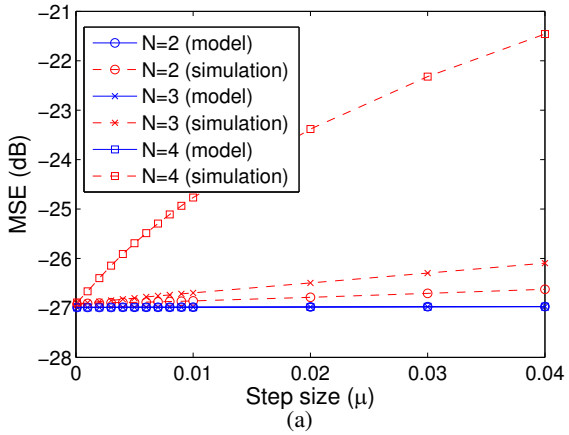

(a)

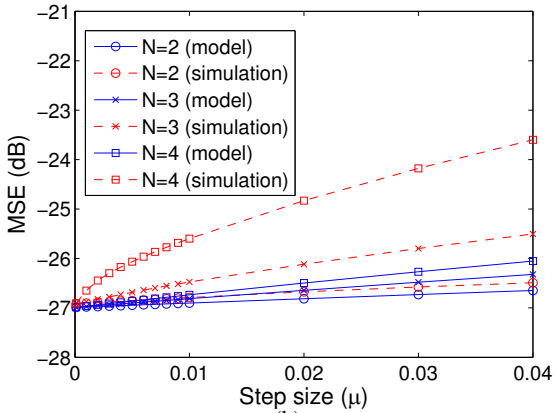

(b)

Figure 4: Comparison between the estimated MSE (a) by (37) for the multichannel FXAP or (b) by (43) for the multichannel MFXAP, and the simulated MSE as a function of μ for different AP orders.

and (b), the theoretical predictions of MSE are not very accurate for high AP orders especially for the FXAP algorithm. Therefore, these results are coherent with [5], [6] where low AP orders were only considered.

5. CONCLUSIONS

In this paper, an analysis of the steady-state MSE performance of the multichannel FXAP and MFXAP algorithms for ANC has been proposed. The methodology applied is based on energy conservation relations avoiding other more restrictive assumptions. It has been shown the estimated MSEs derived are a good prediction of the performance of both algorithms. The estimated steady-state behavior of both algorithms has been validated by means of simulations results provided by a single-channel and a multichannel ANC systems. Finally, the estimated means square error of the multichannel algorithms allows to accurately adjust the configuration settings of the practical systems.

REFERENCES

[1] B. Widrow and S. D. Stearns, *Adaptive Signal Processing*. Englewood Cliffs, NJ, Prentice-Hall, 1985.

[2] S. Haykin, *Adaptive Filter Theory*. Upper Saddle River, NJ, Prentice-Hall, 2002.

[3] M. Bouchard, "Multichannel affine and fast affine projection algorithms for active noise control and acoustic equalization systems," *IEEE Trans. Speech Audio Process.*, vol. 11, 1, pp. 54–60, Jan. 2003.

[4] M. Ferrer, A. Gonzalez, M. de Diego and G. Piñero, "Fast affine projection algorithms for filtered-x multichannel active noise control, " *IEEE Trans. Speech Audio Process.*, accepted to be published (ID: T-ASL-01678-2007).

[5] H. Shin and A. Sayed, "Mean Square performance of a family of affine projection algorithms," *IEEE Trans. Signal Process.*, vol.52, n.1, pp. 90-102, January 2004.

[6] A. Carini and G. Sicuranza, "Transient and steady state analysis of filtered-x affine projection algorithms," *IEEE Trans. Signal Process.*, vol.54, n.2, pp. 665-678, February 2006.

[7] M. Ferrer, A. Gonzalez, M. de Diego and G Piñero, "Mean square analysis of a fast filtered-x affine projection algorithm," in *Proc. ICASSP 2008*, Las Vegas, Abril 2008.